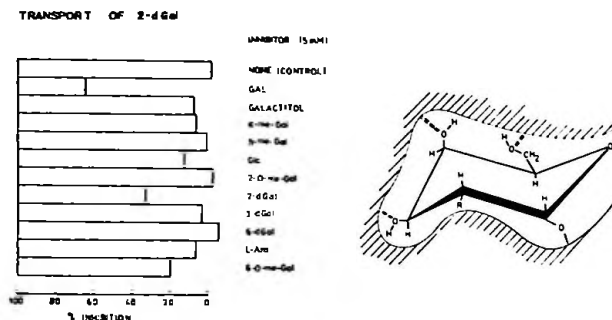


USPHS Grant AM-12619. The authors gratefully acknowledge generous gifts of 3-deoxy-D-galactose (Dr. J.E.G. Barnett, Nottingham, England) and 2-D-methyl-D-galactose (Dr. J. Chittenden, Utrecht, Netherlands).



29 • 1975

### The Specificity of the Transport Systems for Glucose in the renal tubular cells of the Flounder (*Pseudopleuronectes americanus*)

Arnost Kleinzeller, George R. Dubyak and James F. Mullin, University of Pennsylvania School of Medicine, Philadelphia, Pa.

Data on the specificity of both transport pathways for D-glucose found at the antiluminal (basal) face of the renal tubular cells of the winter flounder (*pseudopleuronectes americanus*) have been presented previously (Kleinzeller, and McAvoy, *J. Gen. Physiol.* 62:169, 1973; Kleinzeller, Rittmaster, Griffin and McAvoy, *Bull., Mt. Desert Island Biological Lab.* 14:60, 1974). These studies have been extended using a broader selection of structural analogs of D-glucose. As in previous investigations, an inhibition analysis of model sugars by teased renal tubules served as the principal technique.

Using 0.5 mM methyl-x-D-glucoside-<sup>14</sup>C as a model substrate for the transport system shared by D-glucose and both methyl-D-glucosides, the following newly tested sugars (5 mM) were found to be potent inhibitors: -Fluoro-D-glucose, 3-deoxy-3-fluoro-D-glucose. The sugars -thio-D-glucose and 3-deoxy-D-glucose had no effect. These data, taken in conjunction with previously recorded evidence, indicate that an interaction between the transported sugars and the carrier takes place at the following points: hydrogen bridges may be established between the oxygens at C<sub>1</sub>, C<sub>3</sub> (in the axial configuration) and C<sub>4</sub> (in the equatorial configuration), a pyranose ring structure appears to be essential; finally, a bond of a firmer nature (covalent?) may be formed at C<sub>2</sub>-OH (in the equatorial configuration).

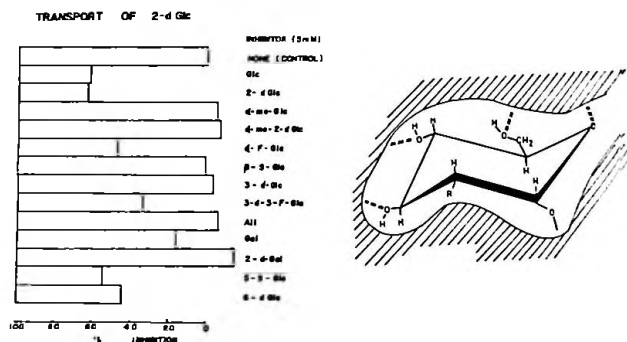
The specificity of the transport pathway shared by D-glucose, 2-deoxy-D-glucose and D-mannose was studied using the last two sugars as models. Figure 1

summarizes data obtained in previous and the present studies by an inhibition analysis of the tissue uptake of 2-deoxy-D-glucose. The inhibition pattern was identical with that for D-mannose and D-glucose (details not given here). Of the newly tested analogs of D-glucose, only -F-glucose, 3-deoxy-F-glucose, 5-thio-glucose and 6-deoxy-glucose were inhibitory. The scheme given in Figure 1 summarizes the possible points of interaction between the carrier and the transported substrates as follows:

A bond of a relatively firm nature (covalent link to a phosphoryl group at the carrier? See Dubyak, Mullin and Kleinzeller, *Bull. Mt. Desert Island Biological Lab* 15:000, 1975) is established at C<sub>1</sub>-OH; fluoride can replace the hydroxyl. Hydrogen bonding at C<sub>3</sub>-OH in the axial configuration is indicated by the fact that 3-deoxy-D-glucose, D-allose and D-altrose were not inhibitory, whereas 3-deoxy-3-F-glucose was inhibitory. C<sub>4</sub>-OH in the equatorial configuration is essential. A pyranose ring structure is mandatory but no hydrogen bond appears to be formed between the ring oxygen and the carrier in the light of the inhibitory effect of 5-thio-D-glucose.

This investigation was supported in part by USPHS Grant AM-12619.

THE Glc-2-dGlc-Man TRANSPORT PATHWAY IN THE FLOUNDER RENAL CELLS



30 • 1975

### Configuration of the Skate (*Raja Erinacea*) Nephron and Ultrastructure of Two Segments of the Proximal Tubule

Eric R. Lacy, Bodil Schmidt-Nielsen, Rainer Galaske and Hilmar Stolte. Mount Desert Island Biological Laboratory, Salsbury Cove, Maine; Medizinische Hochschule Hannover, Germany

The micropuncture study of skate kidney (Stolte *et al.*, *MDIBL Bulletin*, #42, this issue) presented evidence that the principal site of Mg, Phosphate and Sulphate secretion is the proximal tubular segment II (PTS) which is located primarily on the ventral surface of the kidney. Since this is the first time that a specific site of secretion of these divalent ions has been localized, it was of interest to study the ultrastructure of this and other segments of the skate renal nephron. The nephron and

Number of tubular segments in drawing	Sequence of tubular segments	Length of tubular segments in mm	% of total length	Corresponding numbers assigned by Deetjen and Antkoviak
1	1	8	9.8	I & II
2	4	12	14.6	VI
3	6	9	11	VIII
4	2	14	17	III
5	3	25	30.5	IV
6	5	14	17	V
Total			82 mm	100%

Figure 1: Length measurements of the different segments of the skate nephron.

Various parts have previously been described by Deetjen and Antkoviak (*MDIBL Bulletin 10: 5-7, 1970*). In the present study it was examined by *in vivo* dye injection. The passage of the dye was followed by surface microscopy and time lapse photography. Pictures were taken with intervals of 4 to 5 seconds. The various coils of the nephron were also studied by latex injections. From these studies the nephron was reconstructed as shown in Figure 1. Our reconstruction differs in some important respects from that of Deetjen and Antkoviak as shown in Table 1.

Excised tissue was immersed in phosphate buffered glutaraldehyde, postfixed in OsO<sub>4</sub>, dehydrated in graded alcohols and embedded in epoxy resin. One micron thick sections were cut on glass knives, stained with a 1% toluidine blue-1% Borax solution and examined with the light microscope. Thin sections (800A) were cut with Ultratome III on diamond knives, stained with uranyl acetate and lead citrate and examined in a Hitachi HUII-C electron microscope.

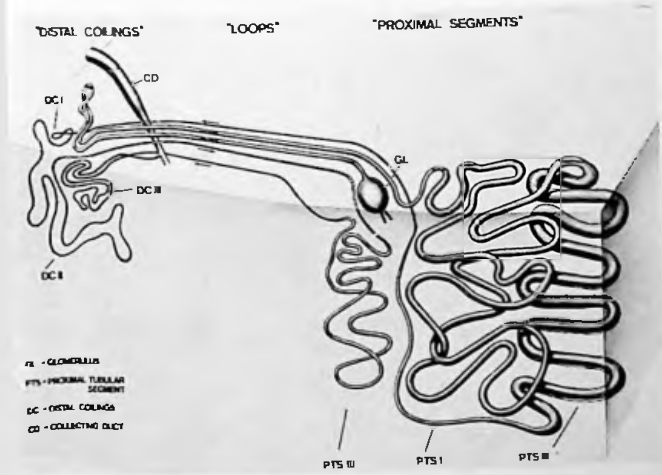


Figure 1: Schematic diagram of the skate nephron showing various segments and their connections.

These will be described in greater detail later. The length of PTS I is about 14 mm, the lumen diameter 35-40 . A few ciliated cells are seen in this segment. The brush border cells are on the average 17 tall and 10 wide (Figure 2). The highly irregular apical plasma membrane with sparse microvilli projects blunt cytoplasmic extensions into the lumen. Membrane bound spheres are present in the tubular lumen. The lateral cell junction has a typical but short terminal bar. Adjacent cells interdigitate along the lateral borders with fingerlike projections oriented perpendicular to the long axis of the cell. The basal membrane is relatively straight and rests on the basal lamina. The basal lamina shows some blunt projections toward the cell. The nucleus is round and centrally located. The most conspicuous cell organelles are numerous, typically shaped mitochondria. These are randomly and rather evenly distributed throughout the cytoplasm, except for a few small microfilaments and a small Golgi apparatus, no other organelles are prominent.

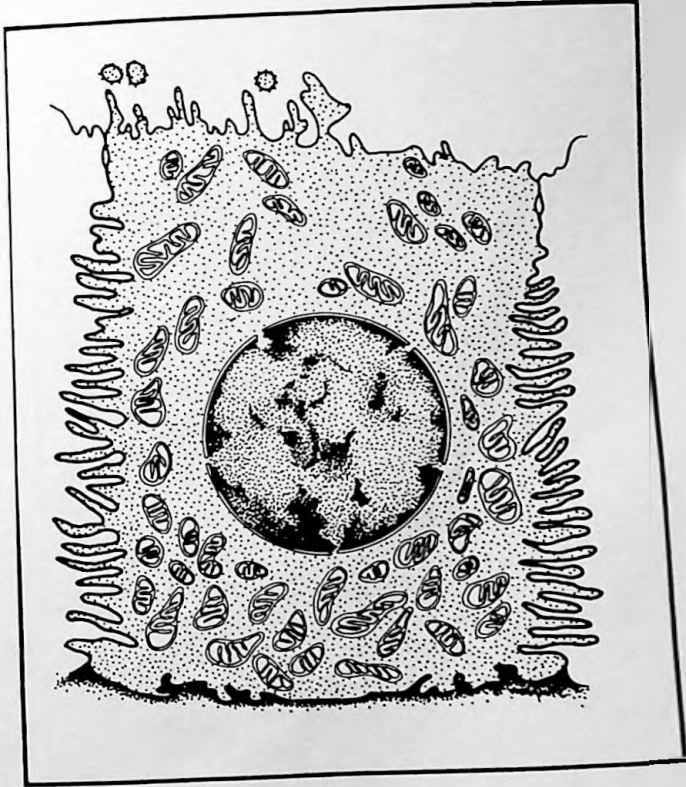


Figure 2: Electron micrograph showing the internal structure of a cell, including a large nucleus and numerous mitochondria.

microvilli are 2-3 times as long as those in PTS I and more densely packed. At the base of some microvilli there appear to be small pinocytotic vesicles. The lateral cell junction has a terminal bar approximately twice as long as that seen in PTS I. The adjacent lateral membranes interdigitate with long fingerlike projections arranged parallel to the long axis of the cell. In contrast to PTS I the lateral membranes are not always closely opposed. Occasional desmosomes are seen on the lateral cell surfaces. The basal membrane rests evenly on the basal lamina which is smooth and appears thinner in PTS I. The round and centrally located nucleus is of the same size as in PTS I. Again the most prominent cell organelles seen are mitochondria which are conspicuously absent just under the apical membrane but otherwise evenly and densely distributed. Rough endoplasmic reticulum and Golgi apparatus are not prominent.

In summary, the segment of the nephron which secretes the divalent ions (PTS II) differs in several respects from PTS I. The cells are much taller, the brush border more pronounced, and lateral cell borders interdigitate in different patterns.

This work was supported by grant DFG (SFB146), AM15972 and General Research Grant (1-SO1RRO5764).

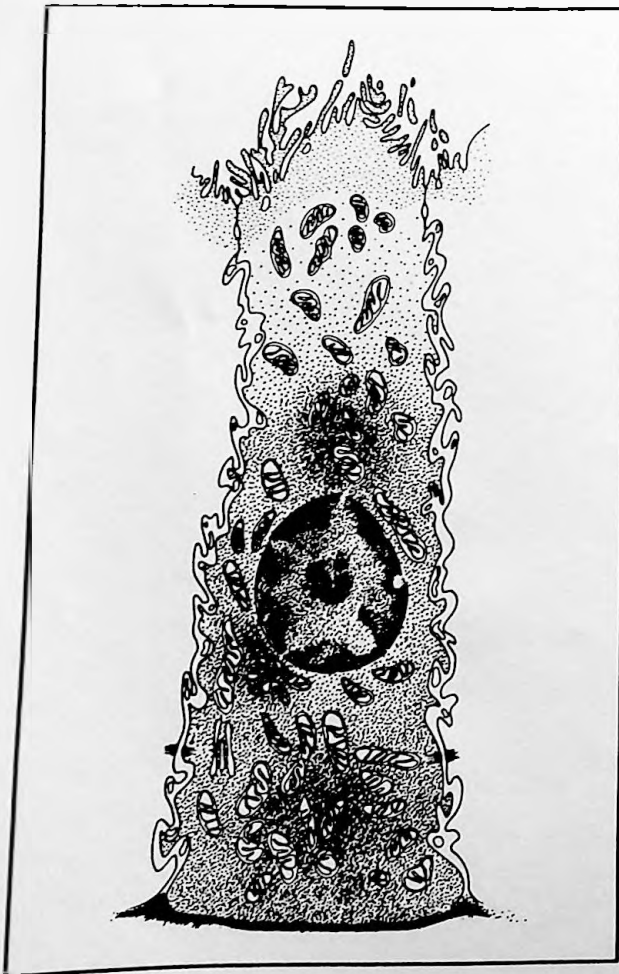


Figure 3

The Urinary Bladder in the Little Skate, *Raja Erinacea*  
 Eric R. Lacy, Bodil Schmidt-Nielsen, Erik Swenson and  
 Thomas Maren. Mount Desert Island Biological Laboratory,  
 Salsbury Cove, Maine, and University of Florida,  
 Gainesville, Florida.

The gross anatomy of the lower urinary tract of the little skate, *Raja erinacea*, was investigated. By injecting phenol red into the tail vein 5-12 hours prior to sacrifice the urine became deeply red or yellow. Only the findings in the female skate will be reported here. The mature female has a distinct, rather large, bilobed urinary bladder (u. bl.) (Figure 1), attached caudally and dorsally to the urogenital sinus (u.s.). It is normally distended with urine (2 to 5 ml). It empties through a short urethra into the urogenital sinus via a small orifice. Eight to ten ureters (Figure 2) lead from each kidney to the dorsal surface of the bladder where they penetrate the epithelium individually. In immature female skates the bladder and urogenital sinus are much smaller. In very young specimens the urine is stored in the cloaca. Urine taken from the bladder of mature female skates is acid (pH 4.50 ± 0.08, n=6), while urine taken from the cloaca of immature specimens is less acid (pH 5.14 ± 0.05, n=4). The difference is significant, P < 0.05.

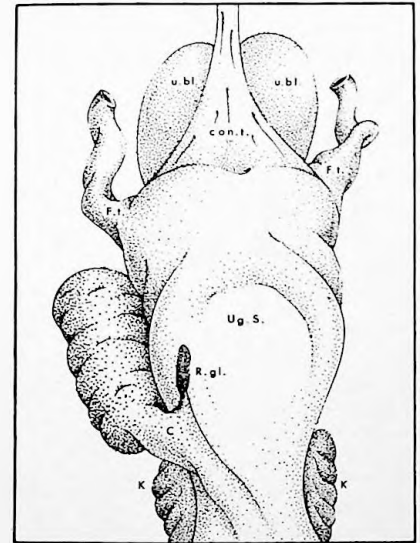


Figure 1

The mucosae of the bladders were dissected and analyzed for carbonic anhydrase content by the micro-method of Maren (*J. Pharm. Expt. Therap.* 130: 1960] using barbital buffer. The tissue contained small definite amounts of enzyme, about 3 units/gram mucosa (on this scale shark red cells have about 40 units/ml). The enzyme activity was entirely abolished by 4 M Metizolamide.

Bladders from mature female skates were removed from the animal and fixed with a phosphate buffered glutaraldehyde-papaformaldehyde fixative, embedded in Epon plastic and sectioned for light and electron